

1 **Impact of Arctic shelf summer stratification on Holocene climate variability**

2

3 Benoit Thibodeau^{1,2,*}, Henning A Bauch³ and Jochen Knies^{4,5}

4

5 ¹Department of Earth Sciences, University of Hong Kong, Pokfulam Road, Hong Kong SAR

6 ²Swire Institute of Marine Science, University of Hong Kong, Cap D'Aguiar, Hong Kong SAR

7 ³Alfred Wegener Institute, Helmholtz Centre for Polar and Marine Research c/o GEOMAR

8 Helmholtz Centre for Ocean Research, Wischhofstrasse 1-3, 24148, Kiel, Germany

9 ⁴Geological Survey of Norway, Trondheim, Norway

10 ⁵CAGE–Centre for Arctic Gas Hydrate, Environment and Climate, Department of Geosciences,

11 UiT The Arctic University of Norway, NO-9037 Tromsø, Norway

12

13

14

15

16 *Correspondence to: Benoit Thibodeau, Department of Earth Sciences, University of Hong

17 Kong, Pokfulam Road, Hong Kong SAR +852 3917 7834 bthib@hku.hk

18

19 Highlights

20

21 • We reconstructed variation in nutrient utilization over the Laptev Sea throughout the
22 Holocene

23 • The Holocene Siberian transgression modulated the water column structure and created
24 unstable conditions until 4 ka

25 • Oceanographic conditions favorable to the onset of the Laptev Sea 'sea-ice factory' were
26 reached around 2 ka

27

28 **Abstract**

29 Understanding the dynamic of freshwater and sea-ice export from the Arctic is crucial to
30 better comprehend the potential near-future climate change consequences. Here, we report
31 nitrogen isotope data of a core from the Laptev Sea to shed light on the impact of the Holocene
32 Siberian transgression on the summer stratification of the Laptev Sea. Our data suggest that the
33 oceanographic setting was less favourable to sea-ice formation in the Laptev Sea during the early
34 to mid-Holocene. It is only after the sea level reached a standstill at around 4 ka that the water
35 column structure in the Laptev Sea became more stable. Modern-day conditions, often described
36 as “sea-ice factory”, were reached about 2 ka ago, after the development of a strong summer
37 stratification. These results are consistent with sea-ice reconstruction along the Transpolar Drift,
38 highlighting the potential contribution of the Laptev Sea to the export of freshwater from the
39 Arctic Ocean.

40

41 **1. Introduction**

42 The Arctic climate is changing at a rapid pace; in fact, this region warms faster than any
43 other on the globe because of polar amplification (Manabe and Stouffer, 1980; Serreze and Barry,
44 2011). One major impact of the observed warming is the dramatic increase in the sea-ice melt
45 season and the consequent reduction of sea-ice cover (Comiso et al., 2008; Perovich and Richter-
46 Menge, 2009). These changes in the sea-ice dynamic directly influence the export of sea-ice via
47 Fram Strait, which accounts for about 25% of the total freshwater export from the Arctic
48 (Serreze et al., 2006). Thus, the Arctic sea-ice export through Fram Strait plays an important role
49 in the global climatic system as it influences the freshwater balance of the northern North
50 Atlantic (Curry, 2005; Sciences et al., 2006), which in turn affects the strength of the Atlantic
51 meridional overturning circulation (Belkin et al., 1998; Dickson et al., 1988; Ionita et al., 2016).

52 From all Siberian shelf seas, the Laptev Sea is thought to contribute the largest fraction of
53 sea-ice export towards Fram Strait (Krumpfen et al., 2016; Reimnitz et al., 1994; Zakharov,
54 1966) (Fig. 1). It was suggested that 20% of the sea-ice transported via the Transpolar Drift
55 (TD) through Fram Strait is produced in the Laptev Sea (Rigor and Colony, 1997) and recent
56 estimates suggested that the Laptev Sea was exporting an area of sea-ice equivalent to 41% of
57 the sea-ice exported via Fram Strait (Krumpfen et al., 2013). Thus, it is critical to understand the
58 longer-term dynamics of sea-ice production within the Laptev Sea in order to better apprehend
59 the potential near-future change in sea-ice export via Fram Strait. The presence of a relatively
60 fresh surface layer promotes the formation of ice in the Laptev Sea, which, in turn, releases
61 brines and contributes to the formation of the shelf halocline layer, a critical “buffer” between
62 the surface and the saltier bottom layer (Dmitrenko et al., 2009; Krumpfen et al., 2013). The
63 resulting stratification is strong enough to persist through the whole year as the long term

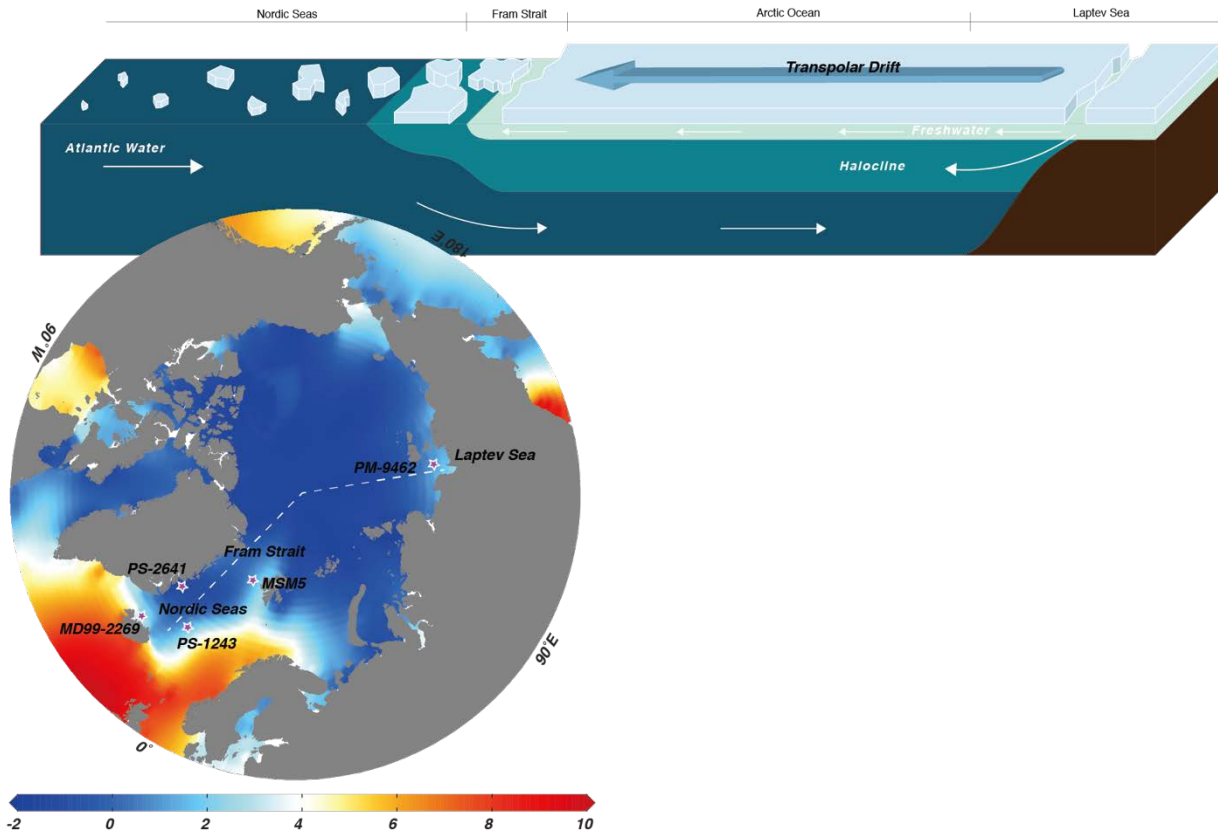
64 probability for winter convection to reach the seafloor is only about 20 % (Dmitrenko et al.,
65 2012; Krumpen et al., 2011). The strength of stratification is controlled by the summer
66 atmospheric circulation that influences the freshwater budget of the Laptev Sea (Dmitrenko et al.,
67 2005, 2008; Thibodeau et al., 2014) and preconditions the next winter sea-ice production (Bauch
68 et al., 2012; Dmitrenko et al., 2010; Thibodeau & Bauch, 2016). Despite the widely recognized
69 climatic importance of the Laptev Sea stratification, we possess no information on its longer-
70 term evolution through the Holocene, i.e., during the past 11 ka when post-glacial sea level rise
71 caused dramatic environmental changes on the circum-arctic shelves (Bauch et al., 2001b), and
72 on the role it might have played on the gradual establishment of modern Arctic climate.

73 Recent work based on geochemical proxies reconstructed the Holocene variability in the
74 production of sea-ice algae over the Laptev Sea (Hörner et al., 2016). They observed a general
75 increasing trend superimposed by short-time variability that was interpreted as representing
76 Bond cycles (1500 ± 500 ka), which are generally considered to be linked to changes in solar
77 activity (Bond et al., 1997). However, the 1500-year cycle in Arctic Oscillation and Arctic sea-
78 ice drift was previously found distinct from the solar irradiance cycle and it was hypothesized
79 that internal variability or indirect response to low-latitude solar forcing was driving the cycle
80 (Darby et al., 2012). This is actually in line with the original analysis of Bond et al (2001) who
81 found the last three ice-drift cycles to be discordant with both the Arctic Oscillation and North
82 Atlantic Oscillation dipole anomaly. This highlight the need to investigate other mechanisms that
83 could influence the sea-ice production in the Arctic Ocean over the Holocene, like water column
84 stratification in marginal seas.

85 Here, we use nitrogen isotope in a well-dated sediment core from the Laptev Sea shelf to
86 reconstruct nutrient utilization and summer stratification. Comparison with proxy of sea-ice

87 algae production is carried-out to investigate the link between the stratification and the variation
88 in sea-ice. We will then implicate our record to sea-ice export, temperature and water
89 stratification proxies along the TD to better understand the potential impact of the Laptev Sea
90 stratification on the larger-scale Arctic climate processes.

91



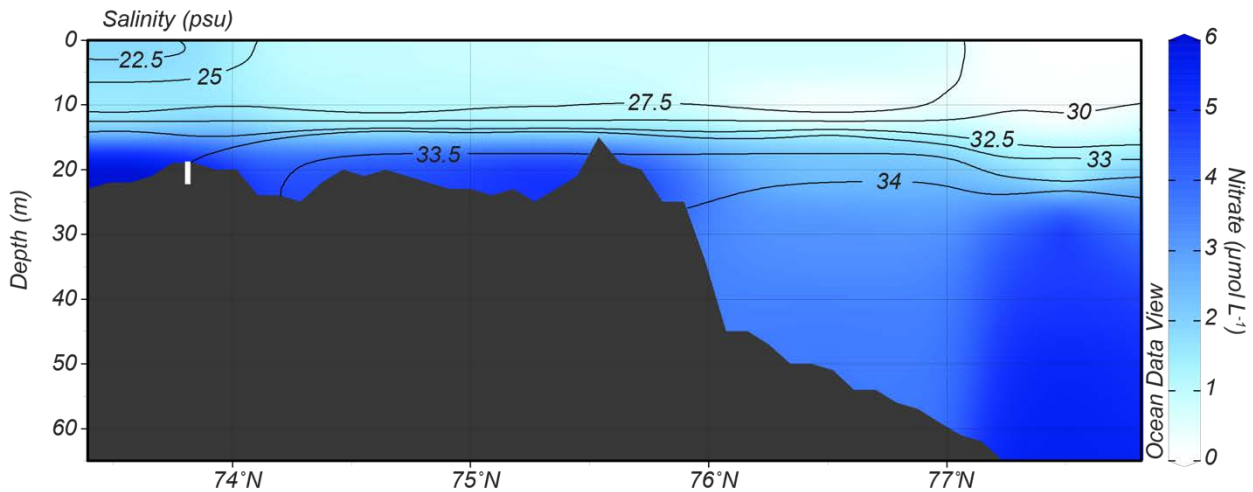
93

94 Fig 1. The Transpolar Drift system from the Laptev Sea to the Nordic Seas. The upper panel is a depth
 95 profile of the different water masses along the white dashed transect on the bottom panel. The color scale
 96 on lower panel shows the 1955-2012-averaged sea-surface January temperature ($^{\circ}\text{C}$) (data from Levitus et
 97 al., 2013). Location of the cores discussed in the paper are indicated by stars on the lower panel.

98

99 **2. Regional Setting**

100 The Laptev Sea is characterized by an estuarine-like circulation, with freshwater runoff from
101 the Lena River at surface and an inflow of salty modified-Atlantic water at depth. This physical
102 feature exerts a strong control on the biogeochemistry of nutrients, notably nitrate (e.g., Kattner
103 et al., 1999). The strong stratification between surface freshwater and marine-derived bottom
104 water prevent any replenishment of nutrients during summer. Thus, nitrate from winter mixing
105 and from the Lena River is rapidly consumed in the surface water during Arctic summer, leading
106 to very low, but not totally depleted, nitrate concentration at the end of the summer ($\sim 0.5 \mu\text{mol}$
107 L^{-1}), while bottom water are between 2 and 6 $\mu\text{mol L}^{-1}$ (Thibodeau et al., 2017a). During winter,
108 mixing occurs and replenishes the surface water with nutrients. The most recent data suggest that
109 the surface water overlying the core today is characterized by nitrate concentration between 1.5
110 and 2 $\mu\text{mol L}^{-1}$ at the end of the Arctic summer (Fig. 2).



111
112 Fig 2. Depth profile of nitrate concentration (color raster) and salinity (black contours) measured in 2014
113 (Thibodeau et al., 2017a) at $\sim 131^\circ\text{N}$, close to the core studied here (represented in white).
114

115 **3. Material and Methods**

116

117 3.1 *Sediment core and chronology*

118 The 467 cm-long vibrocore PM9462 was raised from 27 m water depth in the east part of the
119 Laptev Sea (73°30.2'N, 136°00.3'E). The sediment core was mainly composed of uniform,
120 nearly black, clayey silt (originally described in Bauch et al., 2001b). The chronology of the core
121 was established based on twelve *Portlandia arctica* ¹⁴C measurements (Bauch et al., 2001a).
122 Reservoir age (370 ± 49 ¹⁴C yr B.P.) was determined from the shell of living bivalves from the
123 bottom of the Laptev Sea. Linear interpolation was used to estimate the age between each ¹⁴C
124 value. The oldest measured age is about 8900 cal yr B.P. (Bauch et al., 2001a). Depending on the
125 sample interval, the resolution of each sample ranges from 104 to 391 cal yr.

126

127 3.2 *Geochemical and micropaleontological proxies*

128 Multiples proxies were already available for this sediment core; total organic carbon, δ¹³C or
129 organic carbon, the aquatic palynomorphs (chlorophyceae and dinoflagellates), grain size and
130 garnet content (Fig. 3). Original data and detailed methods can be found in Bauch et al., (2001b).

131

132 3.3 *Organic nitrogen isotope*

133 In this study we use, for the first time, the nitrogen content and nitrogen stable isotope (δ¹⁵N)
134 to investigate the dynamic of nitrogen over this shelf during the Holocene. Nitrogen stable
135 isotope can be used to reconstruct past changes in the nitrogen cycle (e.g., Altabet & Francois,
136 1994; Galbraith et al., 2008; Robinson et al., 2004; Tesdal et al., 2013). In ecosystems where
137 nitrogen is not fully assimilated, the δ¹⁵N is directly linked to the isotopic signature of the supply
138 of nitrate and the fractionation caused by its assimilation and thus, can be used to highlight
139 potential change in the relative proportion of nitrate that is consumed (N-utilization) (Riethdorf

140 et al., 2016; Straub et al., 2013; Thibodeau et al., 2017b). However, in the Arctic Ocean, an
141 important caveat to the use of bulk sediment $\delta^{15}\text{N}$ exists because sediments can contain
142 significant amounts of inorganic nitrogen that includes ammonium adsorbed onto clay minerals
143 (Müller, 1977; Schubert & Calvert, 2001; Stevenson & Dhariwal, 1959). By removing organic
144 nitrogen from the bulk sediment with a KOB_r-KOH solution, it is possible to measure the
145 amount of bound inorganic nitrogen and its isotopic composition (Knies et al., 2007; Schubert
146 and Calvert, 2001). The $\delta^{15}\text{N}$ of the organic nitrogen is then obtained by calculation using the
147 inorganic signal and the bulk $\delta^{15}\text{N}$ in a mass balance equation. This correction removes the
148 potential bias of inorganic nitrogen. Bulk $\delta^{15}\text{N}$ can be altered during burial and early diagenesis,
149 particularly outside of continental margin (Robinson et al., 2012). While it is not possible to
150 unilaterally reject the potential influence of alteration, there is no reasons to suspect large and/or
151 variable alteration of the signal through time as our site was at shallow depth (10 to 30 m)
152 throughout the Holocene (Bauch et al., 2001b). Finally, since our core was located near the coast
153 for the Holocene, we hypothesise that the surface water was never completely limited in nitrate
154 during that period. This is supported by the current setting, where nitrate are not totally used
155 during summer (Fig. 2). It is important to note that the present distance between the core and the
156 coastline is at its maximum for the Holocene, and thus we can suspect that the quantity of
157 nutrient reaching that position is therefore at its minimum for the Holocene. The last factor,
158 beside N-utilization, that could influence our $\delta^{15}\text{N}$ record is the initial signature of the organic
159 material, which can be modified depending on the source of nitrogen (e.g., terrestrial vs marine).
160 Thus, we interpret our $\delta^{15}\text{N}$ record as variation in the ratio of terrestrial to marine organic matter,
161 and/or in a change in N-utilization depending on the information gathered from other proxy.

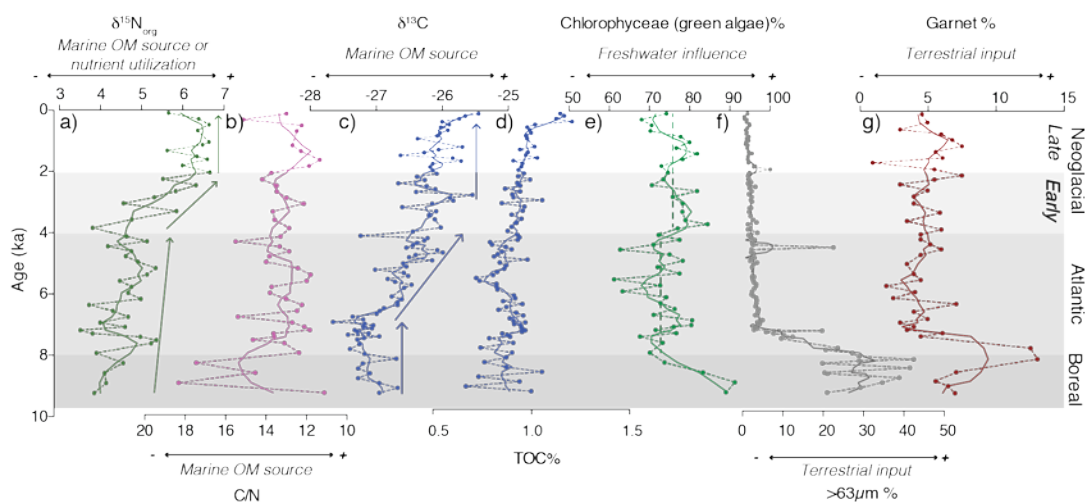
162 Nitrogen content and isotope ratio for both bulk and inorganic nitrogen were analyzed by
163 elemental analyser isotope ratio mass spectrometer (EA-IRMS). The precision for treated and
164 untreated samples was better than ± 0.2 ‰. Organic nitrogen isotope was calculated by
165 subtracting the inorganic value from the bulk isotopic composition (e.g., Knies et al., 2007). The
166 age model and the other proxies for core PM9462 were originally described by Bauch et al.
167 (2001a, 2001b).

168

169 **4. Results**

170 Three distinct periods characterized core PM9462. The bottom of the core (> 8 ka; Boreal
171 period) has a high proportion of terrestrial markers like sand (40%) and garnet (13%), as well as
172 typical terrestrial signatures of $\delta^{13}\text{C}_{\text{org}}$ (-27 ‰) and C:N (>15) (Fig. 3). Sand, C/N ratio and total
173 organic carbon notably show a high degree of variability. This part also has the highest
174 proportion of freshwater algae (>70 to 90 % of total algae content). The $\delta^{15}\text{N}$ of organic nitrogen
175 is slightly higher than 4 ‰. The regime transitions from heavily dominated by terrestrial-markers
176 during the Boreal to more marine-influenced conditions in the Atlantic period (8 to 4 ka); the
177 proportion of sand and garnet decreases dramatically right at the transition and decrease slowly
178 without much variability (sand) or stays constant on average but with a high variability (garnet).
179 The $\delta^{13}\text{C}_{\text{org}}$ starts increasing gradually toward -26 ‰ about 1 ka after the transition, while the
180 C:N ratio drops rapidly to ~ 13 and stays constant on average but with a high variability.
181 Moreover, we observe the lowest proportion of freshwater algae (~ 70 %) and a gradual increase
182 in the isotopic composition of organic nitrogen (Fig. 3). The third period (4 to 0 ka; Neoglacial
183 period) is characterized by relatively constant terrestrial vs marine markers (sand, garnet, $\delta^{13}\text{C}_{\text{org}}$,
184 C:N). However, we could subdivide this period in two parts (early and late) as there is a sharp

185 increase in the $\delta^{15}\text{N}$ around 4 ka and a stabilization (~ 6.5 ‰) at around 2 ka (Fig. 3). The
 186 Neoglacial is also characterized by statistically significant higher freshwater algae (average=
 187 $76.19\% \pm 0.97$, $P < 0.05$; Mann-Whitney test performed with ©Prism7.0d) than the Atlantic
 188 period (average = $72.84\% \pm 1.05$). The freshwater algae record is characterized by high
 189 variability in the Atlantic and Neoglacial periods.
 190



191
 192 Fig 3. Sedimentary proxy in core PM9462 in function of the age model: **a**) $\delta^{15}\text{N}$ of organic nitrogen
 193 (green, in ‰), **b**) carbon to nitrogen ratio (pink), **c**) $\delta^{13}\text{C}$ of the organic carbon (blue, in ‰), **d**) total
 194 organic carbon (blue, in %), **e**) the proportion of green algae (green, in %), **f**) the proportion of sand (grey,
 195 in %) and **g**) the proportion of garnet (red, in %). A 4-neighbors, 2nd order smoothing was applied to all
 196 dataset to see the general trend (solid lines).

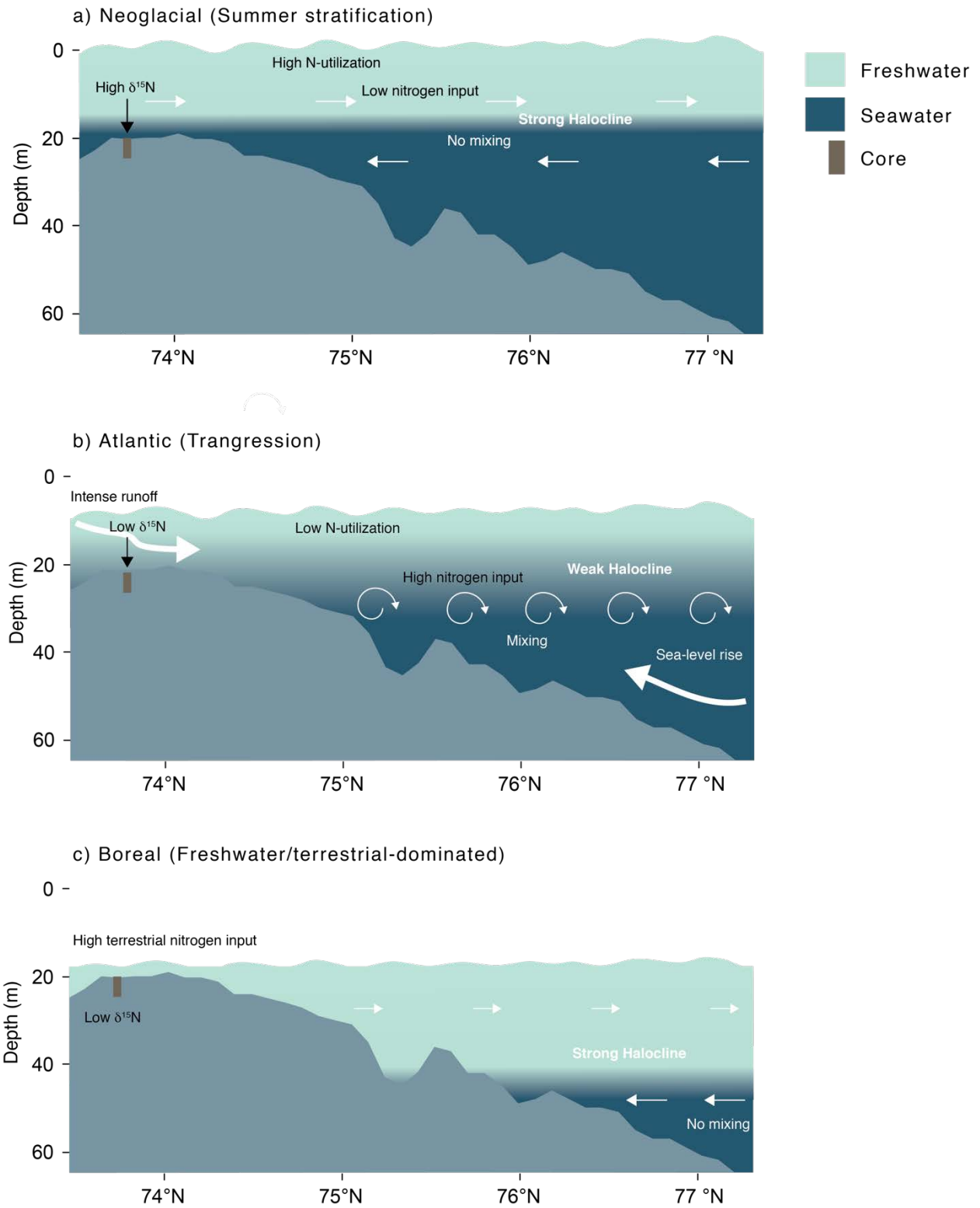
197
 198 **5. Enhanced nitrogen utilization during the Neoglacial**

199 The proxy data from core PM9462 recorded a mixture of two signals: (1) the shift from
 200 terrestrial dominated input to a more marine-influenced organic matter input; (2) change in
 201 nutrient utilization due to change in the water column stratification. The first part of the story is
 202 well documented over the Laptev and Kara Seas (e.g., Bauch et al., 2001a, 1999; Boucsein et al.,

203 2002; Stein et al., 2004, 2001, 1999; Stein and Fahl, 2000). With the initial transgression of the
204 Laptev Sea, a clear transition during the Atlantic period occurred where: (1) most of the geologic
205 marker of detritic input decreased; (2) the freshwater markers decreased; (3) the proportion of
206 marine organic matter increased (Fig. 3). The latter signal is primarily registered in the $\delta^{13}\text{C}_{\text{org}}$
207 record with a trend towards gradually heavier values since c. 7 ka, which is consistent with other
208 geochemical proxies (e.g., Stein et al., 1999). The $\delta^{15}\text{N}_{\text{org}}$ remained largely constant (4 to 5‰)
209 during the Boreal and Atlantic period, highlighting the gradual increase in marine-dominated
210 organic matter from the Boreal to the Atlantic (e.g., Stein et al., 2001). This transition to heavier
211 values might be partially masked by a low N-utilization facilitated by the absence of a strong
212 pycnocline during summer, allowing the mixing of surface water with nutrient rich Atlantic-
213 derived waters (Thibodeau et al., 2017a). The masking effect of N-utilization might explain the
214 small discrepancy between the transition in the early part of the Atlantic periods between $\delta^{15}\text{N}$
215 and the other marine/terrestrial markers (Fig 3). The time between 5 and 8 ka is characterized not
216 only by a constant sea-level rise but also by intense river runoff. That riverine water should have
217 promoted a higher rate of freshwater algae input. However, at our study site we recorded the
218 lowermost amount of these algae during the entire Holocene. A possible explanation for this
219 discrepancy could be that the surface water was slightly saltier than during the Neoglacial. We
220 explain this by suggesting that the intense river runoff combined with the sea-level rise could
221 have created a relatively unstable water column and promoted mixing of surface water with
222 deeper water (Fig. 4). This assumption would be coherent with the irregular sedimentation
223 regime observed during the 5-8 ka period, which was attributed to sea-level rise (Bauch et al.,
224 2001a). This is supported by $\delta^{18}\text{O}$ values from bivalve shells, which found the highest summer
225 salinity value of the Holocene at around 4 ka (Mueller-Lupp et al., 2004). On the other hand,

226 diatoms reconstruction suggest that the Neoglacial was slightly more saline (by about 0.3 psu)
227 compared to the Atlantic period (Polyakova et al., 2005). Irrespective of the proxy used, the
228 difference in salinity between the Atlantic and the Neoglacial seems to have been minor.

229 The transition to the Neoglacial is characterized by a sharp rise in $\delta^{15}\text{N}_{\text{org}}$ during the early
230 part of the period followed by its stabilization at around 2.5 ka. Since the proportions of marine
231 and terrigenous organic matter remained constant during the whole Neoglacial, the sharp rise in
232 the $\delta^{15}\text{N}_{\text{org}}$ record around 4 ka is caused by an increase in the nutrient limitation rather than a
233 change of source of nitrogen. The reason for this sharp increase is likely due to the establishment
234 of a strong summer stratification after sea-level rise came to a standstill and thus, enhanced
235 nutrient utilization in the uppermost water masses in the Laptev Sea shelf (Fig. 4).



236

237 Fig 4. Schematic of our conceptual model for the a) Neoglacial, b) Atlantic and c) Boreal period

238 oceanography of the Laptev Sea shelf. The sediment core PM9462 is represented by the brown rectangle.

239 The **c)** Boreal period was characterized by a high amount of freshwater and high terrestrial input (low
240 $\delta^{15}\text{N}$) due to the proximity of the core to the river mouth. The high input of nutrient was probably also
241 causing low nutrient utilization (low $\delta^{15}\text{N}$). Our coring site was dominated by freshwater. The **b)** Atlantic
242 period was dominated by the transgression, sea-level rises and the gradual increasing influence of marine
243 water at our coring site throughout the period. The gradual increase in marine organic matter drove the
244 slight increase in $\delta^{15}\text{N}$ as the strong mixing due to the transgression probably kept the nutrient utilization
245 low (low $\delta^{15}\text{N}$). Summer stratification was established only during the **a)** Neoglacial, after the sea-level
246 reached a standstill, the strong halocline and decreased riverine input reduced the nitrogen input and
247 increased the nutrient utilization (high $\delta^{15}\text{N}$).

248

249 **6. Evolution of the Laptev Sea stratification and sea-ice export by the Transpolar Drift** 250 **(TD) system during the Holocene**

251 The single most important factor that might control Arctic sea-ice production during the
252 Holocene is the position and the size of large polynyas off Siberia, from which the Laptev Sea is
253 considered the most important being closest to where the TD originates (Krumpfen et al., 2016;
254 Reimnitz et al., 1994; Zakharov, 1966). While changes in sea-ice coverage varied throughout the
255 Holocene (Hörner et al., 2016), the underlying mechanism driving the variability throughout the
256 Holocene is still equivocal. Increase in sea-level during the Holocene should be suspected to
257 have an influence on the configuration on the Laptev Sea ice factory. However, no clear
258 evidence was available to reconstruct the variability of this configuration. Here, we use our
259 reconstruction of the summer stratification as a proxy of favourable condition for sea-ice
260 production in the Laptev Sea and compare the result with a Holocene record of sea-ice algae
261 production from the Laptev Sea and paleoceanographic data from the Atlantic end of the TD (Fig.
262 5).

263

264 6.1 *Boreal and Atlantic (10 to ~ 4 ka)*

265 The postglacial sea-level in the Laptev Sea rose by about 40 m during the Holocene
266 transgression (Bauch et al., 2001b). The data suggest a relatively low nitrate-utilization and that
267 most organic matter originated from land, which is consistent with previous findings using
268 organic geochemical proxies (e.g., Boucsein et al., 2002; Fahl and Stein, 1999; Stein et al., 1999).
269 The latter is also supported by our first-hand approximation of the proportion of terrestrial
270 organic matter based on the $\delta^{13}\text{C}_{\text{org}}$, which suggest that about 87 % of the total organic matter
271 was of terrigenous origin (SOM). That assumption is coherent with the oldest part of the core
272 where the $\delta^{15}\text{N}$ value is similar to the $\delta^{15}\text{N}$ value of particulate organic matter measured in the
273 Lena River (4.6 ‰) (McClelland et al., 2016), corroborating the terrestrial origin of most of the
274 organic matter during this period. During this period the water column was well-mixed with
275 advection of nutrient-rich bottom water on the shelf due to the rapid sea-level rise (8 to 13
276 $\text{mm}\cdot\text{yr}^{-1}$; Bauch et al., 2001b, 2001a). Unstable conditions were also observed in Fram Strait,
277 with a weakly stratified water column and a strong influence of Atlantic water (Werner et al.,
278 2016). During this relatively warm period, very low sea-ice algae production was reconstructed
279 in Fram Strait and on the Greenland and Icelandic shelves based on IP_{25} (Fig 5; Cabedo-Sanz et
280 al., 2016; Müller et al., 2012; Werner et al., 2013). Moreover, the presence of warm Atlantic
281 water was observed at the Reykjanes Ridge, suggesting a weak East Greenland current and a
282 relatively northward positioning of the sub-Arctic front (Moros et al., 2012; Perner et al., 2017).
283 Furthermore, a thin mixed-layer was observed in the Nordic Sea during this period, suggesting a
284 weak import of surface freshwater from the Arctic (Thibodeau et al., 2017b). During the
285 Holocene, modern sea-ice condition over the central Arctic, with a perennial sea-ice cover, was

286 established around 5-8 ka (Cronin et al., 2010; Fahl and Stein, 2012). Thus, during this period,
287 the Laptev Sea was characterized by a mixed water column and conditions unfavorable to intense
288 sea-ice formation. This is illustrated by the slight increase of sea-ice algae production at the
289 beginning of the Atlantic period, which become more important at around 6.5 ka but stays
290 around 50% of the modern-day value (Fig. 5b). Coincidentally, sea-ice export through Fram Strait
291 was minimal, as suggested by the low IRD, and upper-ocean stratification was high in the Nordic
292 Sea, suggesting a thin surface mixed-layer due to weak freshwater export from the Arctic (Fig.
293 5e, h).

294

295 *6.2 Early Neoglacial (~ 4 to 2 ka)*

296 After the sea-level reached its highstand at around 4-5 ka (Bauch et al., 2001a, 2001b), the
297 condition became more stable in the Laptev Sea and a transition phase from the pre-4 ka unstable
298 conditions toward the modern, highly-stratified, oceanographic setting commenced (Fig. 5a).
299 This transition phase was characterized by an increase in nutrient utilization due to the
300 progressive stabilization of the water column and river runoff as suggested by the consistency of
301 most of the proxy data in this part of the core (i.e., no change in the marine to terrestrial ratio of
302 organic matter input; Fig. 3). The ongoing stabilization of the water column here provided
303 increasingly favourable conditions for the formation of polynyas and pack ice. Interestingly,
304 there is no synchronous response in the sea-ice algae production over the Laptev Sea during this
305 period (Fig. 5b). The 1800-year cycle identified in the IP₂₅ record indicates that, at this timescale,
306 there is a strong linkages between sea-ice formation and atmospheric processes like the Arctic
307 and North Atlantic oscillations in the Laptev Sea (Hörner et al., 2016). A similar cycle have been
308 identified in reconstruction of Arctic sea-ice drift during the Holocene (Darby et al., 2012).

309 During the same period, sea-ice cover continuously increased in the high Arctic (e.g., Xiao et al.,
310 2015), Chukchi Sea (Stein et al., 2017), Baffin Bay (e.g., Kolling et al., 2018), Fram Strait (e.g.,
311 Werner et al., 2013) and over the Icelandic shelf (Cabedo-Sanz et al., 2016) but only slightly
312 over the Greenland shelf (Kolling et al., 2017; Müller et al., 2012). While climatic conditions
313 became more favourable for in-situ sea-ice formation in the Arctic and marginal seas, the three-
314 fold increase in IRD in Fram Strait (Werner et al., 2013) suggest a synchronous enhanced sea-ice
315 export from the Arctic (Fig. 5e). Interestingly, the water column in Fram Strait also transitioned
316 to a strongly stratified water column at around 3 ka as indicated by the difference between the
317 $\delta^{13}\text{C}$ values of *Neogloboquadrina pachyderma* sinistral (NPs) and *Turborotalita quinqueloba*
318 (Fig. 5f), with much cooler water at the surface as evidenced by the abundance of NPs (Fig. 5e).
319 That change in stratification was also observed in the Nordic Seas, where the mixed-layer depth
320 increased through this period, suggesting increased flux of freshwater from the Arctic
321 (Thibodeau et al., 2017b). Much cooler surface water was observed over the Icelandic shelf and
322 the Reykjanes Ridge linked with freshwater input and a greater influence of the sub-Arctic front
323 (Cabedo-Sanz et al., 2016; Moros et al., 2012; Perner et al., 2017).

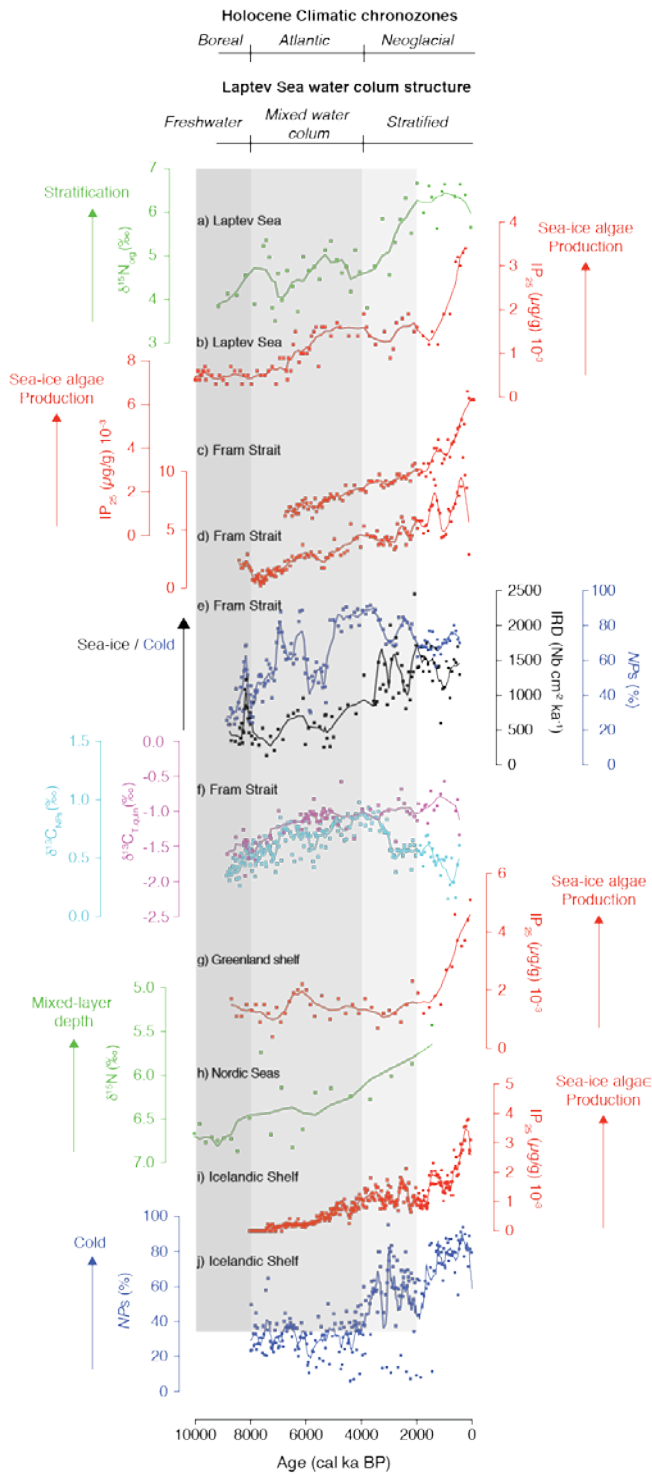
324

325 6.3 Late Neoglacial (2 ka to Recent)

326 The complete stabilization of the modern summer stratification of the Laptev Sea was
327 reached at 2 ka (Fig. 5a). We believe that it is also the onset of the present-day configuration of
328 the so called “sea-ice factory” of the Laptev Sea. This configuration allowed the increase in sea-
329 ice cover suggested by the increase in sea-ice algae production (Fig. 5b). However, the increase
330 was not simultaneous probably because of the decrease observed in the 1800-year cycle in sea-
331 ice cover that is driving most of the short-term sea-ice algae production variability (Hörner et al.,

332 2016). Temperature reconstruction during this period suggests a local trend with warmer surface
333 water and more stratified upper-ocean structure in Fram Strait while the Nordic Seas and the
334 Icelandic shelves are characterized by cooler surface water (Cabedo-Sanz et al., 2016; Thibodeau
335 et al., 2017b; Werner et al., 2013). Sea-ice algae production is generally increasing at all sites
336 (Fram Strait, Greenland and Icelandic shelves), culminating at the end of the record when sea-ice
337 margin reached its southern location (Perner et al., 2017) (Fig. 5). In this part of the record the
338 IRD suggests a constant export of sea-ice from the Arctic to Fram Strait (Fig. 5e). Moreover, a
339 shift in the mineral source region from Arctic to Fjord at around 1.2 ka in core from East
340 Greenland shelf might be related to increased outflow from Fjords and is correlated with glacier
341 advance in Greenland indicating a widespread increase in sea-ice production (Kolling et al.,
342 2017; Solomina et al., 2015).

343



344

345 Fig 5. Reconstruction of **a)** stratification in the Laptev Sea based on $\delta^{15}\text{N}$, **b)** sea-ice algae production in
 346 the Laptev Sea based on IP_{25} (Hörner et al., 2016), **c)** and **d)** sea-ice algae production in Fram Strait
 347 (MSM5-723-2 and 712-2) based on IP_{25} (Müller et al., 2012; Werner et al., 2013), **e)** sea-ice import and

348 subsurface temperature in Fram Strait (MSM5-712-2) based on ice-rafted debris and polar planktic
349 foraminifera *Neogloboquadrina pachyderma* sinistral (NPs) respectively (Werner et al., 2013), **f**)
350 stratification of Fram strait (MSM5-712-2) based on $\delta^{13}\text{C}$ of *Neogloboquadrina pachyderma* sinistral and
351 *Turborotalita quinqueloba* (Werner et al., 2013), **g**) sea-ice algae production over the Greenland shelf
352 (PS2641-4) based on IP₂₅ (Müller et al., 2012), **h**) stratification in the Nordic Seas (PS1243) based on
353 $\delta^{15}\text{N}$ (Thibodeau et al., 2017b), **i**) sea-ice algae production over the Icelandic shelf (MD99-2269) based
354 on IP₂₅, (Cabedo-Sanz et al., 2016), **j**) subsurface temperature over the Greenland shelf (MD99-2269)
355 based on polar planktic foraminifera *Neogloboquadrina pachyderma* sinistral (Cabedo-Sanz et al., 2016).
356 A 4-neighbors, 2nd order smoothing was applied to all dataset to see the general trend (solid lines).

357

358

359 **7. Paleoclimatic Implications**

360 Our results highlight the fact that favorable conditions for sea-ice formation in the Laptev
361 Sea after 2 ka are concomitant to enhanced export of sea-ice via Fram Strait and the installment
362 of modern-like conditions along the TD up to the central Nordic Seas. This also implies a change
363 in the Arctic atmospheric circulation system after the mid-Holocene as it drives the TD. Thus,
364 we suggest that the establishment of a stable water column structure in the Laptev Sea, after the
365 Holocene transgression, had a significant impact on the sea-ice dynamic over the Arctic and on
366 the freshwater export via Fram Strait. This increase in freshwater export probably contributed to
367 regulate climate during the last 2 000 years through its impact on Arctic heat budget and on polar
368 North Atlantic stratification. While more work is needed to disentangle the exact drivers of sea-
369 ice variability throughout the Holocene, we show here that the onset of coastal Arctic sea-ice
370 factory probably played a role, along solar activity, in the production of sea-ice and its export

371 toward the North Atlantic. This needs to be considered when trying to reconstruct Arctic Ocean
372 sea-ice drift and coverage based on paleo-data and/or modelling (e.g., Funder et al., 2011).

373

374 **Acknowledgements**

375 Original data are available in the online supplementary material. Part of this work was funded by
376 DFG through individual research grant awarded to BT (TH1933/1-1) and the Stephen S.F. Hui
377 Trust Fund. JK is supported by the Norwegian Research Council through its Centres of
378 Excellence funding scheme (grant 223259) and Petromaks2 program (grant 255150). The study
379 contributes to the Russian-German "Laptev Sea System" through CATS. We are thankful to
380 Ruediger Stein and one anonymous reviewer for their very constructive comments. We also
381 thank Mandy Wing Kwan So for her assistance with figure 1 and 4 and Kayi Chan for her
382 comments on the manuscript and U. Struck for analytical support.

383

384 **References**

- 385 Altabet, M.A., Francois, R., 1994. Sedimentary nitrogen isotopic ratio as a recorder for surface
386 ocean nitrate utilization. *Global Biogeochem. Cycles* 8, 103–116. doi:10.1029/93GB03396
- 387 Bauch, D., Hölemann, J., Dmitrenko, I., Janout, M., Nikulina, A., Kirillov, S., Krumpfen, T.,
388 Kassens, H., Timokhov, L., 2012. Impact of Siberian coastal polynyas on shelf-derived
389 Arctic Ocean halocline waters. *J. Geophys. Res. Ocean.* 117. doi:10.1029/2011JC007282
- 390 Bauch, H.A., Kassens, H., Erlenkeuser, H., Grootes, P.M., Thiede, J., 1999. Depositional
391 environment of the Laptev Sea (Arctic Siberia) during the Holocene. *Boreas* 28, 194–204.
- 392 Bauch, H.A., Kassens, H., Naidina, O.D., Kunz-Pirrung, M., Thiede, J., 2001a. Composition and
393 flux of Holocene sediments on the eastern Laptev Sea Shelf, Arctic Siberia. *Quat. Res.* 55,
394 344–351. doi:10.1006/qres.2000.2223
- 395 Bauch, H.A., Mueller-Lupp, T., Taldenkova, E., Spielhagen, R.F., Kassens, H., Grootes, P.M.,
396 Thiede, J., Heinemeier, J., Petryashov, V. V., 2001b. Chronology of the holocene
397 transgression at the north siberian margin. *Glob. Planet. Change* 31, 125–139.
398 doi:10.1016/S0921-8181(01)00116-3
- 399 Belkin, I.M., Levitus, S., Antonov, J., Malmberg, S.-A., 1998. “Great Salinity Anomalies” in the
400 North Atlantic. *Prog. Oceanogr.* 41, 1–68. doi:10.1016/S0079-6611(98)00015-9
- 401 Bond, G., Kromer, B., Beer, J., Muscheler, R., Evans, M.N., Showers, W., Hoffmann, S., Lotti-
402 Bond, R., Hajdas, I., Bonani, G., 2001. Persistent solar influence on north atlantic climate
403 during the Holocene. *Science* (80-.). 294, 2130–2136. doi:10.1126/science.1065680
- 404 Bond, G., Showers, W., Cheseby, M., Lotti, R., Almasi, P., DeMenocal, P., Priore, P., Cullen, H.,
405 Hajdas, I., Bonani, G., 1997. A pervasive millennial-scale cycle in North Atlantic Holocene
406 and glacial climates. *Science* (80-.). 278, 1257–1266. doi:10.1126/science.278.5341.1257
- 407 Boucsein, B., Knies, J., Stein, R., 2002. Organic matter deposition along the Kara and Laptev
408 Seas continental margin (eastern Arctic Ocean) during last deglaciation and Holocene:
409 evidence from organic–geochemical and petrographical data. *Mar. Geol.* 183, 67–87.
410 doi:10.1016/S0025-3227(01)00249-3
- 411 Cabedo-Sanz, P., Belt, S.T., Jennings, A.E., Andrews, J.T., Geirsdóttir, Á., 2016. Variability in
412 drift ice export from the Arctic Ocean to the North Icelandic Shelf over the last 8000 years:
413 A multi-proxy evaluation. *Quat. Sci. Rev.* 146, 99–115.
414 doi:10.1016/j.quascirev.2016.06.012
- 415 Comiso, J.C., Parkinson, C.L., Gersten, R., Stock, L., 2008. Accelerated decline in the Arctic sea
416 ice cover. *Geophys. Res. Lett.* 35. doi:10.1029/2007GL031972
- 417 Cronin, T.M., Gemery, L., Briggs, W.M., Jakobsson, M., Polyak, L., Brouwers, E.M., 2010.
418 Quaternary Sea-ice history in the Arctic Ocean based on a new Ostracode sea-ice proxy.
419 *Quat. Sci. Rev.* 29, 3415–3429. doi:10.1016/j.quascirev.2010.05.024
- 420 Curry, R., 2005. Dilution of the Northern North Atlantic Ocean in Recent Decades. *Science* (80-
421 .). 308, 1772–1774. doi:10.1126/science.1109477
- 422 Darby, D.A., Ortiz, J.D., Grosch, C.E., Lund, S.P., 2012. 1,500-year cycle in the Arctic
423 Oscillation identified in Holocene Arctic sea-ice drift. *Nat. Geosci.* 5, 897–900.
424 doi:10.1038/ngeo1629
- 425 Dickson, R.R., Meincke, J., Malmberg, S.-A., Lee, A.J., 1988. The “great salinity anomaly” in
426 the Northern North Atlantic 1968–1982. *Prog. Oceanogr.* 20, 103–151. doi:10.1016/0079-
427 6611(88)90049-3
- 428 Dmitrenko, I., Kirillov, S., Eicken, H., Markova, N., 2005. Wind-driven summer surface

429 hydrography of the eastern Siberian shelf. *Geophys. Res. Lett.* 32.
430 doi:10.1029/2005GL023022

431 Dmitrenko, I., Kirillov, S., Tremblay, L.B., 2008. The long-term and interannual variability of
432 summer fresh water storage over the eastern Siberian shelf: Implication for climatic change.
433 *J. Geophys. Res.* 113. doi:10.1029/2007JC004304

434 Dmitrenko, I.A., Kirillov, S.A., Bloshkina, E., Lenn, Y.D., 2012. Tide-induced vertical mixing in
435 the Laptev Sea coastal polynya. *J. Geophys. Res. Ocean.* 117. doi:10.1029/2011JC006966

436 Dmitrenko, I.A., Kirillov, S.A., Krumpfen, T., Makhotin, M., Povl Abrahamsen, E., Willmes, S.,
437 Bloshkina, E., Hölemann, J.A., Kassens, H., Wegner, C., 2010. Wind-driven diversion of
438 summer river runoff preconditions the Laptev Sea coastal polynya hydrography: Evidence
439 from summer-to-winter hydrographic records of 2007-2009. *Cont. Shelf Res.* 30, 1656–
440 1664. doi:10.1016/j.csr.2010.06.012

441 Dmitrenko, I.A., Kirillov, S.A., Tremblay, L.B., Bauch, D., Willmes, S., 2009. Sea-ice
442 production over the Laptev Sea shelf inferred from historical summer-to-winter
443 hydrographic observations of 1960s–1990s. *Geophys. Res. Lett.* 36, L13605.
444 doi:10.1029/2009GL038775

445 Fahl, K., Stein, R., 2012. Modern seasonal variability and deglacial/Holocene change of central
446 Arctic Ocean sea-ice cover: New insights from biomarker proxy records. *Earth Planet. Sci.*
447 *Lett.* 351–352, 123–133. doi:10.1016/j.epsl.2012.07.009

448 Fahl, K., Stein, R., 1999. Biomarkers as organic-carbon-source and environmental indicators in
449 the Late Quaternary Arctic Ocean: problems and perspectives. *Mar. Chem.* 63, 293–309.
450 doi:10.1016/S0304-4203(98)00068-1

451 Funder, S., Goosse, H., Jepsen, H., Kaas, E., Kjaer, K.H., Korsgaard, N.J., Larsen, N.K.,
452 Linderson, H., Lysa, A., Moller, P., Olsen, J., Willerslev, E., 2011. A 10,000-Year Record
453 of Arctic Ocean Sea-Ice Variability--View from the Beach. *Science* (80-.). 333, 747–750.
454 doi:10.1126/science.1202760

455 Galbraith, E.D., Sigman, D.M., Robinson, R.S., Pedersen, T.F., 2008. Nitrogen in Past Marine
456 Environments, *Nitrogen in the Marine Environment.* doi:10.1016/B978-0-12-372522-
457 6.00034-7

458 Hörner, T., Stein, R., Fahl, K., Birgel, D., 2016. Post-glacial variability of sea ice cover, river
459 run-off and biological production in the western Laptev Sea (Arctic Ocean) – A high-
460 resolution biomarker study. *Quat. Sci. Rev.* 143, 133–149.
461 doi:10.1016/j.quascirev.2016.04.011

462 Ionita, M., Scholz, P., Lohmann, G., Dima, M., Prange, M., 2016. Linkages between atmospheric
463 blocking, sea ice export through Fram Strait and the Atlantic Meridional Overturning
464 Circulation. *Sci. Rep.* 6. doi:10.1038/srep32881

465 Kattner, G., Lobbes, J. M., Fitznar, H. P., Engbrodt, R., Nöthig, E.-M.M., Lara, R. J., 1999.
466 Tracing dissolved organic substances and nutrients from the Lena River through Laptev Sea
467 (Arctic). *Mar. Chem.* 65, 25–39. doi:10.1016/S0304-4203(99)00008-0

468 Knies, J., Brookes, S., Schubert, C.J., 2007. Re-assessing the nitrogen signal in continental
469 margin sediments: New insights from the high northern latitudes. *Earth Planet. Sci. Lett.*
470 253, 471–484. doi:10.1016/j.epsl.2006.11.008

471 Kolling, H.M., Stein, R., Fahl, K., Perner, K., Moros, M., 2018. New insights into sea ice
472 changes over the past 2 . 2 kyr in Disko Bugt , West Greenland. *arktos* 4, 11.
473 doi:10.1007/s41063-018-0045-z

474 Kolling, H.M., Stein, R., Fahl, K., Perner, K., Moros, M., 2017. Short-term variability in late

475 Holocene sea ice cover on the East Greenland Shelf and its driving mechanisms.
476 *Palaeogeogr. Palaeoclimatol. Palaeoecol.* 485, 336–350. doi:10.1016/j.palaeo.2017.06.024
477 Krumpen, T., Gerdes, R., Haas, C., Hendricks, S., Herber, A., Selyuzhenok, V., Smedsrud, L.,
478 Spreen, G., 2016. Recent summer sea ice thickness surveys in Fram Strait and associated ice
479 volume fluxes. *Cryosphere* 10, 523–534. doi:10.5194/tc-10-523-2016
480 Krumpen, T., Holemann, J. a., Willmes, S., Morales Maqueda, M. a., Busche, T., Dmitrenko, I. a.,
481 Gerdes, R., Haas, C., Heinemann, G., Hendricks, S., Kassens, H., Rabenstein, L., Schröder,
482 D., 2011. Sea ice production and water mass modification in the eastern Laptev Sea. *J.*
483 *Geophys. Res. C Ocean.* 116, 1–17. doi:10.1029/2010JC006545
484 Krumpen, T., Janout, M., Hodges, K.I., Gerdes, R., Girard-Arduin, F., Hölemann, J.A., Willmes,
485 S., 2013. Variability and trends in Laptev Sea ice outflow between 1992–2011. *Cryosph.* 7,
486 349–363. doi:10.5194/tc-7-349-2013
487 Levitus, S., Antonov, J.I., Baranova, O.K., Boyer, T.P., Coleman, C.L., Garcia, H.E., Grodsky,
488 A.I., Johnson, D.R., Locarnini, R.A., Mishonov, A. V., Reagan, J.R., Sazama, C.L., Seidov,
489 D., Smolyar, I., Yarosh, E.S., Zweng, M.M., 2013. The World Ocean Database. *Data Sci. J.*
490 12, WDS229-WDS234. doi:10.2481/dsj.WDS-041
491 Manabe, S., Stouffer, R.J., 1980. Sensitivity of a global climate model to an increase of CO₂
492 concentration in the atmosphere. *J. Geophys. Res.* 85, 5529–5554.
493 doi:10.1029/JC085iC10p05529
494 McClelland, J.W., Holmes, R.M., Peterson, B.J., Raymond, P.A., Striegl, R.G., Zhulidov, A. V.,
495 Zimov, S.A., Zimov, N., Tank, S.E., Spencer, R.G.M., Staples, R., Gurtovaya, T.Y., Griffin,
496 C.G., 2016. Particulate organic carbon and nitrogen export from major Arctic rivers. *Global*
497 *Biogeochem. Cycles* 30, 629–643. doi:10.1002/2015GB005351
498 Moros, M., Jansen, E., Oppo, D.W., Giraudeau, J., Kuijpers, A., 2012. Reconstruction of the
499 late-Holocene changes in the Sub-Arctic Front position at the Reykjanes Ridge, north
500 Atlantic. *The Holocene* 22, 877–886. doi:10.1177/0959683611434224
501 Mueller-Lupp, T., Bauch, H.A., Erlenkeuser, H., 2004. Holocene hydrographical changes of the
502 eastern Laptev Sea (Siberian Arctic) recorded in $\delta^{18}\text{O}$ profiles of bivalve shells. *Quat. Res.*
503 61, 32–41. doi:10.1016/j.yqres.2003.09.003
504 Müller, J., Werner, K., Stein, R., Fahl, K., Moros, M., Jansen, E., 2012. Holocene cooling
505 culminates in sea ice oscillations in Fram Strait. *Quat. Sci. Rev.* 47, 1–14.
506 doi:10.1016/j.quascirev.2012.04.024
507 Müller, P.J., 1977. C/N ratios in Pacific deep-sea sediments: Effect of inorganic ammonium and
508 organic nitrogen compounds sorbed by clays. *Geochim. Cosmochim. Acta* 41, 765–776.
509 doi:10.1016/0016-7037(77)90047-3
510 Perner, K., Moros, M., Jansen, E., Kuijpers, A., Troelstra, S.R., Prins, M.A., 2017. Subarctic
511 Front migration at the Reykjanes Ridge during the mid- to late Holocene: evidence from
512 planktic foraminifera. *Boreas*. doi:10.1111/bor.12263
513 Perovich, D.K., Richter-Menge, J.A., 2009. Loss of Sea Ice in the Arctic. *Ann. Rev. Mar. Sci.* 1,
514 417–441. doi:10.1146/annurev.marine.010908.163805
515 Polyakova, Y.I., Bauch, H.A., Klyuvitkina, T.S., 2005. Early to middle Holocene changes in
516 Laptev Sea water masses deduced from diatom and aquatic palynomorph assemblages. *Glob.*
517 *Planet. Change* 48, 208–222. doi:10.1016/j.gloplacha.2004.12.014
518 Reimnitz, E., Dethleff, D., Nürnberg, D., 1994. Contrasts in Arctic shelf sea-ice regimes and
519 some implications: Beaufort Sea versus Laptev Sea. *Mar. Geol.* 119, 215–225.
520 doi:10.1016/0025-3227(94)90182-1

- 521 Riethdorf, J.R., Thibodeau, B., Ikehara, M., Nürnberg, D., Max, L., Tiedemann, R., Yokoyama,
522 Y., 2016. Surface nitrate utilization in the Bering sea since 180 kA BP: Insight from
523 sedimentary nitrogen isotopes. *Deep. Res. Part II Top. Stud. Oceanogr.* 125–126, 163–176.
524 doi:10.1016/j.dsr2.2015.03.007
- 525 Rigor, I., Colony, R., 1997. Sea-ice production and transport of pollutants in the Laptev Sea,
526 1979–1993. *Sci. Total Environ.* 202, 89–110. doi:https://doi.org/10.1016/S0048-
527 9697(97)00107-1
- 528 Robinson, R.S., Brunelle, B.G., Sigman, D.M., 2004. Revisiting nutrient utilization in the glacial
529 Antarctic: Evidence from a new method for diatom-bound N isotopic analysis.
530 *Paleoceanography* 19, 1–13. doi:10.1029/2003PA000996
- 531 Robinson, R.S., Kienast, M., Luiza Albuquerque, A., Altabet, M., Contreras, S., De Pol Holz, R.,
532 Dubois, N., Francois, R., Galbraith, E., Hsu, T.C., Ivanochko, T., Jaccard, S., Kao, S.J.,
533 Kiefer, T., Kienast, S., Lehmann, M., Martinez, P., McCarthy, M., Möbius, J., Pedersen, T.,
534 Quan, T.M., Ryabenko, E., Schmittner, A., Schneider, R., Schneider-Mor, A., Shigemitsu,
535 M., Sinclair, D., Somes, C., Studer, A., Thunell, R., Yang, J.Y., 2012. A review of nitrogen
536 isotopic alteration in marine sediments. *Paleoceanography* 27. doi:10.1029/2012PA002321
- 537 Schubert, C.J., Calvert, S.E., 2001. Nitrogen and carbon isotopic composition of marine and
538 terrestrial organic matter in Arctic Ocean sediments: *Deep Sea Res. Part I Oceanogr. Res.*
539 *Pap.* 48, 789–810. doi:10.1016/S0967-0637(00)00069-8
- 540 Sciences, C., Brunswick, N., Agency, A., Watershed, S., Hole, W., Seitzinger, S., Harrison, J. a,
541 Böhlke, J.K., Bouwman, a F., Lowrance, R., Peterson, B., Tobias, C., Van Drecht, G., 2006.
542 Denitrification across landscapes and waterscapes: a synthesis. *Ecol. Appl.* 16, 2064–90.
- 543 Serreze, M.C., Barrett, A.P., Slater, A.G., Woodgate, R.A., Aagaard, K., Lammers, R.B., Steele,
544 M., Moritz, R., Meredith, M., Lee, C.M., 2006. The large-scale freshwater cycle of the
545 Arctic. *J. Geophys. Res. Ocean.* 111. doi:10.1029/2005JC003424
- 546 Serreze, M.C., Barry, R.G., 2011. Processes and impacts of Arctic amplification: A research
547 synthesis. *Glob. Planet. Change* 77, 85–96. doi:10.1016/j.gloplacha.2011.03.004
- 548 Solomina, O.N., Bradley, R.S., Hodgson, D.A., Ivy-Ochs, S., Jomelli, V., Mackintosh, A.N.,
549 Nesje, A., Owen, L.A., Wanner, H., Wiles, G.C., Young, N.E., 2015. Holocene glacier
550 fluctuations. *Quat. Sci. Rev.* doi:10.1016/j.quascirev.2014.11.018
- 551 Stein, R., Boucsein, B., Fahl, K., Garcia de Oteyza, T., Knies, J., Niessen, F., 2001.
552 Accumulation of particulate organic carbon at the Eurasian continental margin during late
553 Quaternary times: Controlling mechanisms and paleoenvironmental significance. *Glob.*
554 *Planet. Change* 31, 87–104. doi:10.1016/S0921-8181(01)00114-X
- 555 Stein, R., Dittmers, K., Fahl, K., Kraus, M., Matthiessen, J., Niessen, F., Pirrung, M., Polyakova,
556 Y., Schoster, F., Steinke, T., Fütterer, D.K., 2004. Arctic (palaeo) river discharge and
557 environmental change: Evidence from the Holocene Kara Sea sedimentary record, in:
558 *Quaternary Science Reviews.* pp. 1485–1511. doi:10.1016/j.quascirev.2003.12.004
- 559 Stein, R., Fahl, K., 2000. Holocene accumulation of organic carbon at the Laptev Sea continental
560 margin (Arctic Ocean): sources, pathways, and sinks. *Geo-Marine Lett.* 20, 27–36.
561 doi:10.1007/s003670000028
- 562 Stein, R., Fahl, K., Niessen, F., Siebold, M., 1999. Late Quaternary organic carbon and
563 biomarker records from the Laptev Sea continental margin (Arctic Ocean): implications for
564 organic carbon flux and composition, in: *Land-Ocean Systems in the Siberian Arctic:*
565 *Dynamics and History.* pp. 635–655.
- 566 Stein, R., Fahl, K., Schade, I., Manerung, A., Wassmuth, S., Niessen, F., Nam, S. II, 2017.

567 Holocene variability in sea ice cover, primary production, and Pacific-Water inflow and
568 climate change in the Chukchi and East Siberian Seas (Arctic Ocean). *J. Quat. Sci.* 32, 362–
569 379. doi:10.1002/jqs.2929

570 Stevenson, F.J., Dhariwal, A.P.S., 1959. Distribution of fixed ammonium in soils. *Soil Sci. Soc.*
571 *Am. J.* 23, 121–125.

572 Straub, M., Tremblay, M.M., Sigman, D.M., Studer, A.S., Ren, H., Toggweiler, J.R., Haug, G.H.,
573 2013. Nutrient conditions in the subpolar North Atlantic during the last glacial period
574 reconstructed from foraminifera-bound nitrogen isotopes. *Paleoceanography* 28, 79–90.
575 doi:10.1002/palo.20013

576 Tesdal, J.E., Galbraith, E.D., Kienast, M., 2013. Nitrogen isotopes in bulk marine sediment:
577 Linking seafloor observations with subseafloor records. *Biogeosciences* 10, 101–118.
578 doi:10.5194/bg-10-101-2013

579 Thibodeau, B., Bauch, D., 2016. The impact of climatic and atmospheric teleconnections on the
580 brine inventory over the Laptev Sea shelf between 2007 and 2011. *Geochemistry, Geophys.*
581 *Geosystems* 17, 56–64. doi:10.1002/2015GC006063

582 Thibodeau, B., Bauch, D., Kassens, H., Timokhov, L.A., 2014. Interannual variations in river
583 water content and distribution over the Laptev Sea between 2007 and 2011: The Arctic
584 Dipole connection. *Geophys. Res. Lett.* 41, 7237–7244. doi:10.1002/2014GL061814

585 Thibodeau, B., Bauch, D., Voss, M., 2017a. Nitrogen dynamic in Eurasian coastal Arctic
586 ecosystem: Insight from nitrogen isotope. *Global Biogeochem. Cycles* 31.
587 doi:10.1002/2016GB005593

588 Thibodeau, B., Bauch, H.A., Pedersen, T.F., 2017b. Stratification-induced variations in nutrient
589 utilization in the Polar North Atlantic during past interglacials. *Earth Planet. Sci. Lett.* 457,
590 127–135. doi:10.1016/j.epsl.2016.09.060

591 Werner, K., Müller, J., Husum, K., Spielhagen, R.F., Kandiano, E.S., Polyak, L., 2016. Holocene
592 sea subsurface and surface water masses in the Fram Strait: Comparisons of temperature
593 and sea-ice reconstructions. *Quat. Sci. Rev.* 147, 194–209.
594 doi:10.1016/j.quascirev.2015.09.007

595 Werner, K., Spielhagen, R.F., Bauch, D., Hass, H.C., Kandiano, E., 2013. Atlantic Water
596 advection versus sea-ice advances in the eastern Fram Strait during the last 9 ka: Multiproxy
597 evidence for a two-phase Holocene. *Paleoceanography* 28, 283–295.
598 doi:10.1002/palo.20028

599 Xiao, X., Stein, R., Fahl, K., 2015. MIS 3 to MIS 1 temporal and LGM spatial variability in
600 Arctic Ocean sea ice cover: Reconstruction from biomarkers. *Paleoceanography* 30, 969–
601 983. doi:10.1002/2015PA002814

602 Zakharov, V.F., 1966. The role of flaw leads off the edge of fast ice in the hydrological and ice
603 regime of the Laptev Sea. *Oceanology* 6, 815–821.
604
605